OPTIMIZATION OF SOLAR PV SMOOTHING ALGORITHMS FOR REDUCED STRESS ON A UTILITY-SCALE BATTERY ENERGY STORAGE SYSTEM

W. Greenwood[1], O. Lavrova[2], A. Mammoli[1], F. Cheng[2], S. Willard[3]
[1]Department of Mechanical Engineering, [2]Department of Electrical and Computer Engineering
University of New Mexico, Albuquerque, New Mexico 87131
[3]Public Service Company of New Mexico (PNM)

With the increase in grid-tied utility-scale solar PV energy production, there is a growing concern for distributed power variability due to high-frequency intermittency caused by clouds and other atmospheric obstructions. Using battery energy storage, power can be "smoothed" before being dispatched to the grid by calculating the smoothed profile of the raw power, then charging or discharging storage to achieve all or part of this difference in profile. There are many algorithms for calculating the smoothed profile, each providing varying smoothing quality in terms of ramp rate reduction and battery stress which shortens the lifespan causing increased system O&M costs. In this analysis, modeled system behaviors using three smoothing algorithms, including one which simulates a short-term power forecast, are compared for battery stress under equivalent ramp rate reduction performance. Results show that battery stress is most significantly reduced when using a centered moving average algorithm which utilizes the short-term prediction.

Keywords: optimization, PV, smoothing, battery storage

INTRODUCTION

Grid-tied utility-scale solar photovoltaic (PV) distributed energy production is becoming more prevalent thanks to increasing affordability and improved performance of equipment. While this provides many benefits regarding sustainability and future grid structure, it creates new challenges for power quality regulation. PV power can change nearly instantaneously due to passing scattered clouds and other atmospheric obstructions. Large fluctuations in grid power can disrupt distribution by causing flicker and overall inconsistent power which can lead to penalties against utility companies. Currently, changes in power are typically mitigated with the use of load tap changer (LTC) operations which keep an acceptable range of voltage. However, the increase in distributed PV power generation introduces more instances where an LTC operation is required, thus inflicting more wear on the equipment and possibly increasing O&M and equipment replacement costs.

High-frequency intermittency can also be addressed on-site with generation through smoothing which involves using fast-response energy storage to dampen severe power ramps before electricity is dispatched onto the grid [1]. This is done by calculating the smoothed profile of the raw PV power, then charging or discharging storage appropriately to achieve all or part of this difference in profile. There are many algorithms for calculating this smoothed profile and they provide varying quality of smoothing in terms of ramp rate (change in power) reduction, stress on energy storage, and system requirements for making the calculation. In the case of a battery energy storage system (BESS), increased stress shortens the lifespan leading to increased system O&M and replacement costs. The goal of this analysis is to determine which of three different smoothing algorithms inflicts minimal BESS stress while providing equivalent smoothing performance, thus optimizing the batteries' longevity. Knowing this, one can tailor algorithm operation parameters to provide the desired reduction of ramp rates.

This analysis was performed using, in part, historical power data (before and after smoothing) from the Prosperity Energy Storage Project near Mesa del Sol in Albuquerque, New Mexico shown in figure 1 [2]. This DOE/ARRA funded SMART Grid Storage Project is investigating large-scale grid-tied PV energy production with utility-scale battery storage capable of simultaneous load shifting and smoothing [3]. The pre-smoothing (raw) power data were used to numerically model the theoretical power output which was then calibrated to the Prosperity's historical post-smoothing pri-

mary meter (PM) power data.

Figure 1: Prosperity Energy Storage Project near Mesa del Sol in Albuquerque, New Mexico which has 500kW PV capacity with BESS capable of simultaneous shifting and smoothing.

The numerical model used for this analysis was produced by modifying a model used by Sandia National Laboratories for an unrelated study [4]. The modifications included introducing a third algorithm which simulates a perfect short-term solar power forecast. Running each algorithm for the project's one-second temporal resolution PV power data, theoretical ramp rate distributions and BESS usage characteristics are compared side by side for algorithms using a low pass filter, lagging moving average, or centered moving average (simulating a short-term solar forecast). Prior to algorithm comparison, parameters such as deadband and system response delays are calibrated to adequately reproduce historical output data from the Prosperity Site for days using either lagging moving average or low pass filter real-time.

THEORY

Algorithms

The first step to apply PV power smoothing is to determine a goal output power value which closely follows solar resource while removing high-frequency intermittency. The difference between the smooth profile and raw power are then mitigated by the BESS to achieve the desired output. The smooth profile is calculated based on a span of real-time raw PV power data. Two common algorithms for calculating this smoothing profile are a moving average (MA) and low pass filter (LPF). A moving average is the mean of all data within a user-determined time window (tw) either immediately before (lagging) or around (centered) the current time stamp. A LPF is a means of removing variability at frequencies below the cut-off frequency represented by the time constant (tc). Example smoothed profiles resulting from the lagging MA, centered MA and LPF based on real data are shown in figure 2.

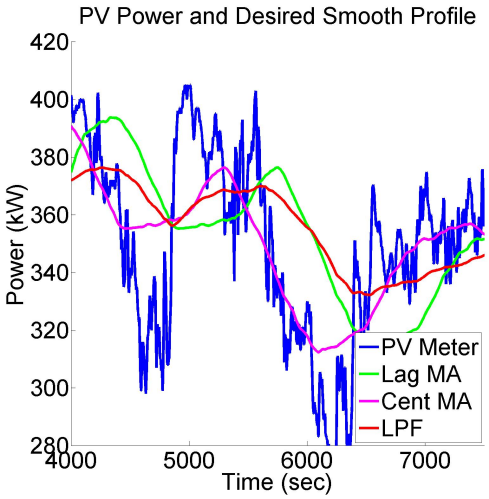

Figure 2: Model smoothed power profiles by which battery operation is determined; note characteristics in different algorithms.

The lagging MA has the advantage of utilizing only known past data but exhibits a delay in profile causing larger differences in raw and desired power. The LPF offers a seemingly flatter profile but also creates some considerable differences which the battery storage would need to mitigate. A centered MA yields a profile which best follows the real-time power, however this method requires knowledge of future power obtained from a short-term forecast. In this study actual data is used to simulate a forecast even though a real forecast would have a degree of error. Regardless, this provides a means to evaluate the potential for short-term forecasting to reduce battery stress.

Applied Smoothing

In real world application smoothing is imperfect causing the net output to maintain some variability greater than that of the smooth profile. This can be due to unintentional factors such as control system or battery response delays which can magnify power ramps if there is a sudden ramp in the opposite direction from the previous time stamp.

Net output can also deviate unintentionally due to load at the power station as required by heating or cooling causing ramps outside of the algorithm's visibility. Lastly, unforeseen ramps can be introduced after applied smoothing when the power, which is smoothed at residential/commercial voltage (e.g. 480 V), is passed through the step-up transformer to transmission voltage levels (e.g. 12.47 kV). This effect was experienced during this analysis and addressed by utilizing data only from meters on the low side of the transformer.

Deviation can also be user controlled in an attempt to prevent unnecessary battery use while maintaining desired smoothing quality. A deadband is a ramp rate value below which smoothing will not be applied because the ramp is deemed not significant enough to justify mitigation. For the Prosperity Site a 20 kW deadband is utilized and thus used for the algorithms tested here. Likewise, though algorithms tested in this study attempt to smooth 100% of power ramps, smoothing can be applied to mitigate a percentage of ramps as long as output is satisfactory. Perhaps the simplest way to control smoothing quality is to adjust the MA's time window or LPF's time constant. Increasing these values produce a flatter goal power profile but also increases BESS use. These factors in applied smoothing yield a smoothed output power as shown in figure 3 for the profiles shown previously in figure 2.

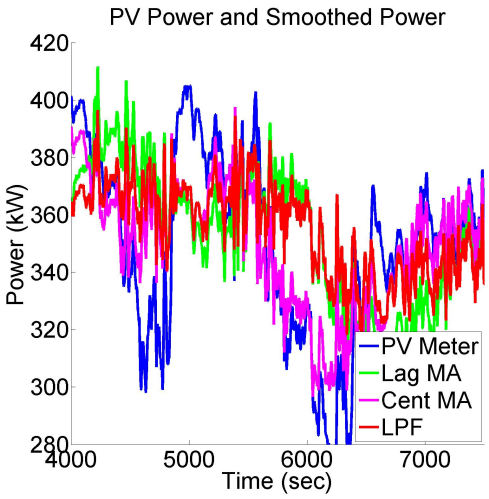

Figure 3: Model smoothed power with applied smoothing characteristics caused by system delays and smoothing deadband.

Though there are many factors affecting smoothing quality, the goal in this study was to establish equality among the algorithms which is shown by ramp rate distribution, mean ramp rates, and 99th percentile ramp rates. All ramp rates were calculated using an absolute value two-point backwards difference. This allows comparison to be made with regards to battery stress which is represented by the running total of displaced energy and frequency response figures. The end-of-day total displaced energy values for each algorithm are then compared to quantify usage.

RESULTS

Ramp Rate Reduction

Matching the model's user-defined parameters to those used at the Prosperity Site, sufficiently equivalent smoothing quality was exhibited among the three algorithms. The ramp rate distribution in figure 4 shows the three algorithms to be visually identical and this behavior was found to be consistent for all data sets evaluated. The distribution shown is zoomed to a window which removes lower ramps in order to increase high-magnitude ramp visibility though distributions overlapped at lower ramps as well.

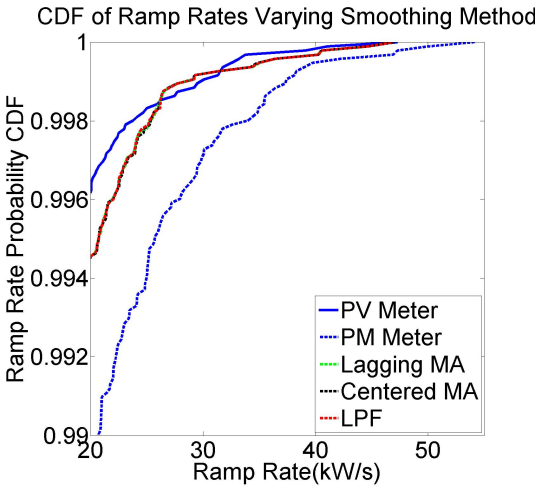

Figure 4: Distribution of ramp rates for historical and algorithm power signals; looking for equivalent performance among algorithms.

Note that historical smoothed power data experienced worse ramps after smoothing. This is attributed to noise introduced by the step-up transformer as mentioned in the theory section. The mean ramp rate for each data set shown in this figure is shown in table 1.

Table 1: Mean ramp rates for net outputs modeled using 1/3/12 data set; note roughly equivalent values among algorithms.

Algorithm	Mean Ramp Rate (W/s)
Lagging MA	508.62
Cenetered MA	513.29
LPF	508.20

Among the algorithms, the mean ramp rates are sufficiently close to each other to establish equality. However, the centered MA would suggest a slightly higher quantity of maximum ramp rates. To quantify this higher-magnitude ramp rate probability, the 99th percentile ramp rates are shown in table 2. Again the algorithms' values show roughly equivalent smoothing quality.

Table 2: 99th percentile ramp rates for net outputs modeled using 1/3/12 data set; note roughly equivalent values among algorithms; equality consistent for all data sets.

Algorithm	Ramp Rate (kW/s)
Lagging MA	4.00
Cenetered MA	4.04
LPF	4.00

BESS Stress: Energy Displacement

With equivalent smoothing quality established, the algorithms can be compared based on battery stress. This is first presented by a running sum of energy displaced (charged or discharged) by the BESS to smooth the historic raw PV power signal from three different data sets. These days had varying degrees of intermittency as shown by the maximum and mean raw PV ramp rates listed in table 3.

Table 3: Maximum and mean raw PV power ramp rates for time periods used for analysis.

Date (M/D/Y)	Max Ramp Rate (kW/s)	Mean Ramp Rate (kW/s)
1/3/12	10.19	0.50
2/11/13	47.28	2.75
12/18/12	87.10	1.22

The first of these data sets (1/3/12) experienced the lowest magnitude maximum ramp and least sustained variability as seen from the mean ramp rate. It also showed the greatest contrast in performance among the algorithms with respect to energy displaced as shown in figure 5.

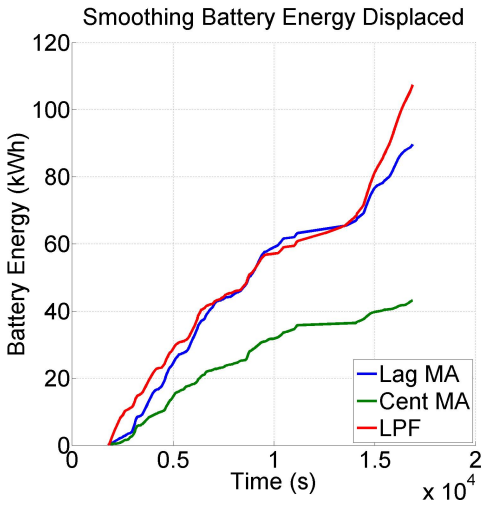

Figure 5: Running sum energy dispatched by BESS as result of smoothing for a moderately intermittent time period (1/3/12).

The next data set (2/11/13) experienced a mid-range maximum ramp rate but significantly more sustained variability. In figure 6 note the reduced advantage of any algorithm over another. The centered MA still exhibits better performance but it's margin is greatly reduced due to the sustained higher-magnitude variability. Despite the reduction, the advantage is still significant and could translate into long-term reduced BESS wear and O&M costs.

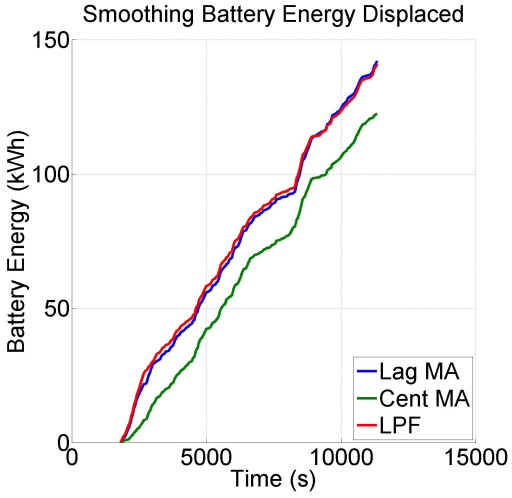

Figure 6: Running sum energy dispatched by BESS as result of smoothing for a highly intermittent time period; note reduced advantage of any algorithm over another (2/11/13).

The final data set (12/18/12) experienced the

highest magnitude maximum ramp rate but lacked the sustained variability experienced during the 2/11/13 data set. However, it's energy displacement curves reinforce the results shown in figure 5 showing a slight advantage of lagging MA over LPF. This behavior is repeated in figure 7 and, again, the centered MA performs best overall.

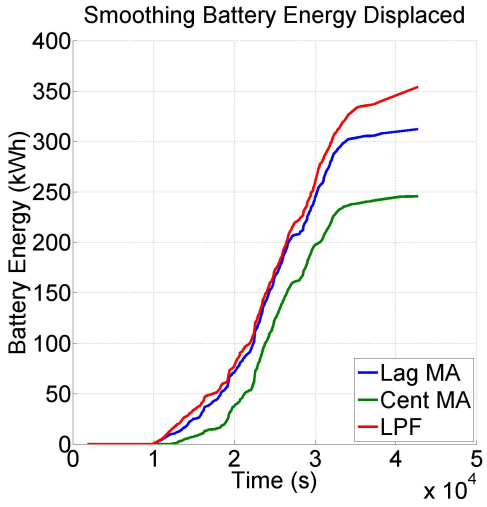

Figure 7: Running sum energy dispatched by BESS as result of smoothing for a highly intermittent time period (12/18/12).

Visually, these three data sets provide impressions for each algorithms behavior. To aid in drawing conclusions, the end total displaced energy by the BESS using each algorithm and the percentage with respect to the worst performing algorithm are also displayed. First consider table 4 which shows the totals for the 1/3/12 data set.

Table 4: BESS energy displaced and percent of worst case for each algorithm during 1/3/12 data set; worst case shows 100%.

Algorithm	Disp. Energy (kWh)	Percent of Worst Case
Lagging MA	89.75	83.51
Cenetered MA	43.14	40.13
LPF	107.48	100

As with figure 5, the numerical results for 1/3/12 show the potential for the centered MA which displaced 40% of the energy that the worst case did. Even though the centered MA's percentage increases with increased intermittency, this outcome is still noteworthy. This sort of intermittency may be the most common in particular climates. Low to moderate intermittency would also be more common for either higher-capacity PV arrays which have a larger footprint or dispersed smaller arrays because they would experience geographic smoothing [5, 6]. Either case would lead to larger BESS stress savings which would better justify increased investment costs for forecasting equipment and technology.

The numerical results for the 2/11/13 data set reveal an outcome not apparent in figure 6. The total displaced energy was largest for the lagging MA closely followed by the LPF. This 0.8% difference may be interpreted as negligible, thus resulting in equivalent performance, but testing of new data sets may reveal this outcome to be significant. The centered MA, though not as advantageous as before, provides a 14% energy displacement reduction.

Table 5: BESS energy displaced and percent of worst case for each algorithm during 2/11/13 data set; worst case shows 100%.

Algorithm	Disp. Energy (kWh)	Percent of Worst Case
Lagging MA	142.2	100
Cenetered MA	122.4	86.1
LPF	141.0	99.2

The final data set (12/18/12) further demonstrates dependency on mean ramp rate as shown in table 6. The LPF inflicted the most stress on the battery while the lagging and centered MAs followed at percentages slightly higher than in table 4. Based on these three data sets' totals, there is a definite dependancy on mean ramp rate as opposed to maximum ramp rate.

Table 6: BESS energy displaced and percent of worst case for each algorithm during 12/18/12 data set; worst case shows 100%.

Algorithm	Disp. Energy (kWh)	Percent of Worst Case
Lagging MA	312.5	88.2
Cenetered MA	245.6	69.4
LPF	354.3	100

BESS Stress: Frequency Response

Total energy displacement provides insight into charge/discharge cycles experienced by the BESS, but stress is also caused by rate of change

and frequency of power flow in and out of the batteries. The frequency response plots of ramp rates are useful to visualize smoothing quality, but it can also used here to show BESS activity. Figure 8 shows the frequency response of the historic battery activity data and battery activity resulting from the three algorithms for the 1/3/12 data set.

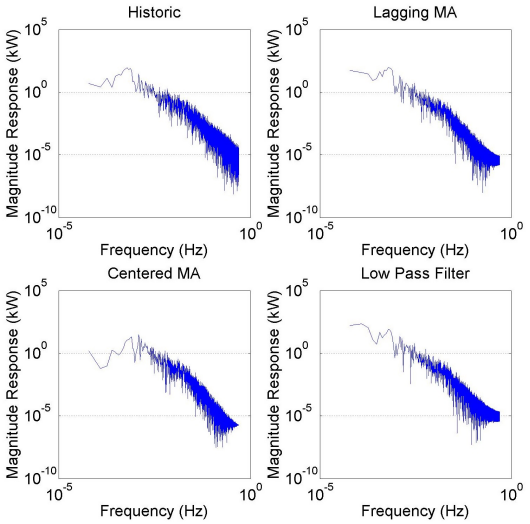

Figure 8: Frequency response of historic and model battery activity as a result of smoothing.

The figures exhibit similar magnitude to historical data. The lagging MA, particularly, correlates well which is to be expected because the historical data set from 1/3/12 utilized the lagging MA smoothing algorithm. Deviation exists at higher frequencies which can be attributed to the noise introduced by system delays and the step-up transformer.

Comparing the three algorithms, the frequency response suggests reduced high-frequency activity for the centered MA. This is represented in the far right area of the frequency response curve which lands at a magnitude of 10^{-6} kW for the centered MA whereas the lagging MA and LPF land at or around 10^{-5} kW.

CONCLUSIONS

Current results suggest that a centered moving average algorithm utilizing a short-term solar forecast provides an advantage over a conventional lagging moving average or low-pass filter due to significantly reduced stress on the batteries for roughly equivalent reduction in ramp rates. Though the simulated forecast used actual data which would correlate to a perfect forecast, the results still show the potential for PV power forecasts to optimize the benefits of PV power production with battery energy storage. Modern solar forecasting methods, however, are still under development and require added system investments such as ground imagery equipment and calibration.

Between conventional methods, some results show lagging moving average to be slightly less battery-intensive for, again, comparable smoothing quality. This apparently superior performance may be dependent on the type of intermittency as is evident in figure 5 where the lagging moving average and low pass filter curves cross over at one point. Moreover, the advantage of any algorithm over another is highly dependant on the degree of variability experienced. This is apparent by the curves' positions relative to each from figure 5 to figure 6.

FUTURE WORK

Currently there are many ways in which this work could be improved to provide higher value conclusions. For example, results show significantly better performance in terms of battery stress when using a short-term power forecast. However, these results were obtained using actual data which correlate to a perfect forecast. For a more plausible performance comparison, this analysis could incorporate error into the forecasted power data to then be used in the centered MA. Alternatively, an actual short-term forecast could be implemented if resources are available. Methods for short-term power forecasting currently in development are showing promise to provide useful results [7].

Another means of improvement could be representing smoothing quality in terms of number of utility ramp rate violations. Presently, there is no formally stated ramp rate magnitude warranting legal or financial repercussions in the continental United States though increased distribution of PV power generation will likely prompt one in the future. For the purposes of this study the requirements could be adopted as published by the Puerto Rico Electric Power Authority (PREPA) which limits ramps to 10% of plant capacity per minute [8]. This is lower frequency than the pri-

mary concern of this analysis but may provide a real-world metric by which the algorithm can be measured. Lastly, smoothing quality can be evaluated by number of LTC operations due to net output ramp rates. This is useful because it represents a real concern for increased wear on utility equipment leading to added O&M costs.

References

[1] Thomas D Hund, Sigifredo Gonzalez, and Keith Barrett. Grid-tied pv system energy smoothing. In *Photovoltaic Specialists Conference (PVSC), 2010 35th IEEE*, pages 002762–002766. IEEE, 2010.

[2] Public service company of new mexico (pnm) prosperity energy storage project. `http://www.pnm.com/systems/docs/prosperity_energy_storage_factsheet2013.pdf`, 2013.

[3] Feng Cheng, Steve Willard, Jonathan Hawkins, Brian Arellano, Olga Lavrova, and Andrea Mammoli. Applying battery energy storage to enhance the benefits of photovoltaics. In *Energytech, 2012 IEEE*, pages 1–5. IEEE, 2012.

[4] Jay Johnson, Abraham Ellis, Atsushi Denda, Kimio Morino, Takao Shinji, Takao Ogata, and Masayuki Tadokoro. Pv output smoothing using a battery and natural gas-engine generator. Technical report, Sandia National Laboratories (SNL-NM), Albuquerque, NM (United States), 2013.

[5] M Sengupta. Measurement and modeling of solar and pv output variability. In *Proc. Solar*, 2011.

[6] Matthew Lave, Jan Kleissl, and Ery Arias-Castro. High-frequency irradiance fluctuations and geographic smoothing. *Solar Energy*, 86(8):2190–2199, 2012.

[7] Chi Wai Chow, Bryan Urquhart, Matthew Lave, Anthony Dominguez, Jan Kleissl, Janet Shields, and Byron Washom. Intra-hour forecasting with a total sky imager at the uc san diego solar energy testbed. *Solar Energy*, 85(11):2881–2893, 2011.

[8] Matthew Lave and Jan Kleissl. Cloud speed impact on solar variability scaling–application to the wavelet variability model. *Solar Energy*, 91:11–21, 2013.